

# The Role of the Transient Outward Current in Action Potential Repolarization: a Simulation Study

Beatriz Carbonell<sup>1</sup>, Lázló Virág<sup>2</sup>, Norbert Jost<sup>2</sup>, András Varró<sup>2</sup>, Chema Ferrero<sup>1</sup>

<sup>1</sup> Grupo de Bioelectrónica (GBIO), I3BH, Universidad Politecnica de Valencia, Valencia, España

<sup>2</sup> Department of Pharmacology & Pharmacotherapy, University of Szeged, Hungary

## Abstract

*The potassium transient outward current ( $I_{to}$ ) is active only during the early plateau of the action potential (AP) and, therefore, its role in governing APD is controversial. The goal of this work is to characterize  $I_{to}$  from patch-clamp experiments in canine ventricular epicardial cells and demonstrate its influence in cardiac restitution using an AP mathematical model. Data from our experiments has been used to define a new mathematical model for  $I_{to}$ , which has been then inserted in the Decker et al. model for canine epicardial AP, substituting the original formulation of  $I_{to}$ . The new model predicts an increase in action potential duration (APD) when  $I_{to}$  is blocked, in accordance with recent experimental evidence. Inspection of the ionic currents in the simulations show that the blockade of  $I_{to}$  may indirectly affect other plateau ionic currents like L-type Calcium current ( $I_{CaL}$ ) and the rapid component of the rectifier potassium current ( $I_{Kr}$ ), producing an increment in the APD. These novel findings emphasize the importance of  $I_{to}$  in repolarization and suggest a potential role of  $I_{to}$  blockade in arrhythmogenesis.*

## 1. Introduction

Ventricular fibrillation is the leading cause of sudden cardiac death. Recent experimental evidences have suggested that fibrillation is created and sustained by the property of restitution of the cardiac action potential duration (APD) [1]. The cardiac transient outward  $K^+$  current ( $I_{to}$ ) activates at the end of the depolarization phase and recovers rapidly from inactivation in dog and human, thus it plays an important role only at the beginning of the action potential (AP), contributing to phase I repolarization and the AP notch [2]. However, the influence of  $I_{to}$  in APD is controversial and depends on the experimental conditions, the region of the myocardium or the species studied. It has been suggested that alterations in  $I_{to}$  may affect the plateau voltage, and consequently, it can indirectly influence the activation and deactivation of certain plateau currents producing a lengthening or a shortening of the APD [3].

Recent experiments using the action potential voltage clamp technique [2] demonstrated that APD significantly lengthens when  $I_{to}$  is blocked using chromanol 293B in the presence of 0.5  $\mu$ M of HMR 1556 (specific blocker of  $I_{Ks}$ ). Furthermore, early afterdepolarizations (EADs) appeared when 0.1  $\mu$ M dofetilide was added to block  $I_{Kr}$  and the cycle length (CL) was increased to 3 s.

In this work, whole-cell patch-clamp experiments were performed to define a new mathematical model of  $I_{to}$ . The new formulation of the potassium transient current was inserted in the canine AP model of Decker et al. [4], replacing the original one. Then, the experimental conditions of [2] were reproduced simulating the effects of the different drugs by partially blocking different ionic currents. The APs and the ionic currents were registered and analyzed to clarify the contribution of the  $I_{to}$  in cardiac repolarization.

## 2. Materials and methods

### 2.1. Whole cell patch clamp experiments

All experiments were carried out in compliance with the *Guide for the Care and Use of Laboratory Animals* (USA NIH publication NO 85-23, revised 1985). The protocols were approved by the Review Board of the Committee on Animal Research of the Animal Health and Animal Welfare Directorate (15.1/01031/006/2008).

Ventricular myocytes were enzymatically dissociated from dog hearts using the segment perfusion technique as described earlier in detail [5]. The protocols followed to fabricate the micropipettes and to carried out the measurements are described in [2], as well as, the detailed containing of the HEPES-buffed Tyrode solution.

When measuring potassium currents, 1  $\mu$ M nisoldipine (gift from Bayer AG, Leverkusen, Germany) was added to the external solution to eliminate L-type  $Ca^{2+}$  current ( $I_{CaL}$ ). The slow component of the delayed rectifier potassium current ( $I_{Ks}$ ) was inhibited by using the selective  $I_{Ks}$  blocker HMR 1556 (0.5  $\mu$ M). In some experiments the rapid component of the delayed rectifier potassium current ( $I_{Kr}$ ) was blocked by 0.1  $\mu$ M dofetilide.

Membrane currents were recorded with Axopatch-1D and 200B patch-clamp amplifiers (Axon Instruments, Union City, CA, USA) using the whole-cell configuration of the patch-clamp technique, following the technique described in [2].

## 2.2. Model

The recently published Decker et al. model [4], both in its original form and using our modified version of  $I_{to}$ , was used to reproduce the experiments carried out in [2]. The Decker model is based on a previous canine AP dynamic model by Hund-Rudy [6], but it incorporates an improved description of intracellular calcium dynamics by including recent finding [7].

The Decker et al. dynamic model [4] contains mathematical descriptions for 16 transmembrane currents (CTKCl,  $K^+$ -Cl $^-$  cotransporter; CTNaCl,  $Na^+$ -Cl $^-$  cotransporter;  $I_{NaL}$ , slowly activating late  $Na^+$  current;  $I_{Na}$ ,  $Na^+$  current;  $I_{Nab}$ , background  $Na^+$  current;  $I_{NaCa}$ ,  $Na^+$ / $Ca^{2+}$  exchanger;  $I_{Cab}$ , background  $Ca^{2+}$  current;  $I_{pCa}$ , sarcolemmal  $Ca^{2+}$  pump;  $I_{to}$ , 4-aminopyridine-sensitive transient outward current;  $I_{Kr}$ , fast component of delayed rectifier  $K^+$  current;  $I_{Ks}$ , slow component of delayed rectifier  $K^+$  current;  $I_{K1}$ , time-dependent  $K^+$  current;  $I_{NaK}$ ,  $Na^+$ - $K^+$  pump current;  $I_{leak}$ , network sarcoplasmic reticulum (NSR) leak current;  $I_{to2}$ ,  $Ca^{2+}$  dependent transient outward Cl $^-$  current;  $I_{CaL}$ , L-type  $Ca^{2+}$  current) and intracellular calcium handling processes ( $I_{diff}$ , ion diffusion, myoplasm-to-SR subspace;  $I_{tr}$ ,  $Ca^{2+}$  transfer, NSR to junction sarcoplasmic reticulum (JSR);  $I_{rel}$ , JSR release current;  $I_{diff,ss}$ , ion diffusion, subspace-to-local ICaL subspace;  $I_{NaCa,ss}$ ,  $Na^+$ / $Ca^{2+}$  exchanger localized to SR subspace).

In some of our simulations, we have modified the formulation of the 4-aminopyridine-sensitive transient outward current ( $I_{to}$ ) as described below.

## 3. Results and discussion

### 3.1. Experimental results

The whole-cell patch-clamp experimental results showed in Figure 1 reveal two main aspects that differ from the present knowledge of  $I_{to}$ . The first is the crossover between the steady-state activation and inactivation curves shown in Figure 1A. The second is the increase of the slow component of the time constant of inactivation.

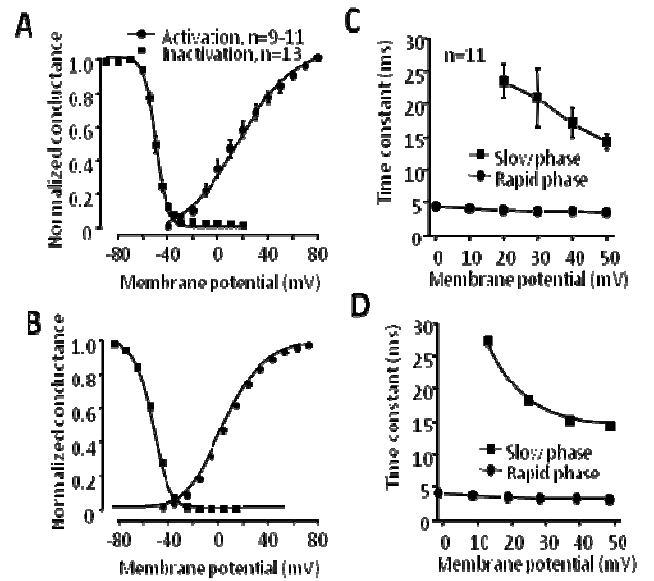


Figure 1. Characterization of the kinetic properties of  $I_{to}$ . (A) Experimental steady-state activation and inactivation curves obtained for  $I_{to}$  in canine ventricular myocytes. (B) Fitted steady-state activation and inactivation curves using Boltzmann functions. (C) Time constants of inactivation were determined by fitting a sum of two exponential functions to the decay phase of  $I_{to}$ . (D) Simulation of the slow and the rapid phase of the inactivation.

### 3.2. Model of $I_{to}$

The data presented in the previous section was used to formulate a new mathematical model for  $I_{to}$ . As in the original Decker et al. model [4], the  $I_{to}$  is formulated as:

$$I_{to} = G_{to} a^3 i_f i_s (V - E_K)$$

where  $G_{to}$  is the maximum conductance,  $a$  is the activation gate,  $i_f$  and  $i_s$  are the fast and slow inactivation gates respectively,  $V$  is membrane potential and  $E_K$  is the Nernst potential for  $K^+$  ions.

The steady-state curves for the gates were reformulated using the data shown in Figure 1A. Experimental data were fitted with Boltzmann functions (Figure 1B) yielding the following equations:

$$a_{\infty} = \frac{1}{1 + \exp\left(-\frac{V + 14.65}{19.78}\right)} \quad i_{f,\infty} = i_{s,\infty} = \frac{1}{1 + \exp\left(\frac{V + 40.08}{8.496}\right)}$$

The new formulation of the steady-state curves produces a slight reactivation of  $I_{to}$  (96 nA/ $\mu$ F) in a range of potentials of -20 and -40 mV. Using the data of Figure 1C, the inactivation time constant was modified obtaining

the curves showed in Figure 1D and the equations:

$$\alpha_{is} = \frac{1}{800 \left[ 1 + \exp\left(\frac{V+60}{5}\right) \right]} \quad \beta_{is} = \frac{1}{15 \left[ 1 + \exp\left(-\frac{V-18}{9}\right) \right]}$$

$$\alpha_{if} = \frac{1}{150 \left[ 1 + \exp\left(\frac{V+58}{5}\right) \right]} \quad \beta_{if} = \frac{1}{5 \left[ 1 + \exp\left(-\frac{V+19}{9}\right) \right]}$$

$$\tau_{is} = \frac{1}{\alpha_{is} + \beta_{is}} \quad \tau_{if} = \frac{1}{\alpha_{if} + \beta_{if}}$$

In the original model, the time constant of inactivation has a value of 10 ms for a membrane potential of 25 mV, while in the modified model it is approximately 25 ms.

### 3.3. Action potential model

Recent experimental evidence shows that the blockade of  $I_{to}$  (together with  $I_{Ks}$ ) increases APD in canine ventricular tissue (Figure 2A). We used the Decker model, both with the original  $I_{to}$  (see Figure 2B) and with the modified  $I_{to}$  (Figure 2C) to try to reproduce and explain this effect. The cell was stimulated by a train containing 200 identical pulses at 1 Hz (amplitude twice diastolic threshold) until it reached steady-state. Three types of simulations were carried out: control, 100%  $I_{Ks}$  block (simulating the effect of HMR 1556 [2]) and 100%  $I_{Ks}$  block + 90%  $I_{to}$  block (simulating the effect of Chromanol 293B [2]), respectively.

Figure 2B shows the results obtained using the original Decker et al. [4]. When  $I_{Ks}$  was fully blocked, APD does not change significantly compared to the control situation, what is consistent with the experimental results (Figure 2A). However, additional  $I_{to}$  inhibition (90%) shifts the early plateau to more positive voltages and eventually shortens APD in 10% (Figure 2B), in contrast with the experimental results. Conversely, the same simulations using the modified  $I_{to}$  model correlated well with the experimental data of [2], and the inhibition of  $I_{to}$  in presence of full block of  $I_{Ks}$  produced APD prolongation (Figure 2C).

In order to understand why APD increases in the presence of  $I_{to}$  inhibition, the main ionic currents underlying the AP were monitored during the simulations.  $I_{Kr}$  and  $I_{CaL}$  turned out to be the plateau currents more affected by changes in  $I_{to}$ . The traces of these currents during the AP, in control conditions and under the effect of a 100%  $I_{Ks}$  blockade and under the effects of 100% and 90% blockade of  $I_{Ks}$  and  $I_{to}$ , respectively, are shown in Figure 3. A detailed analysis of Figure 3 clarifies that there are three factors cooperating in slowing down repolarization in the mid-plateau in  $I_{to}$  block conditions compared to control in the modified Decker et al. [4] model. The first is the higher value of  $I_{Kr}$  in the modified control model compared to the modified  $I_{to}$  block model, as shown in Figure 3D. The second is an increment in  $I_{CaL}$  produced when the  $I_{to}$  is blocked (Figure 3B, lower inset), a fact that increases the inward balance of currents and rises membrane potential. The third is the late activation of  $I_{to}$  at the beginning of repolarization in control conditions due to the “window” current (Figure 3B, upper inset), which is a consequence of the overlap of the steady-state activation and inactivation curves in the new formulation of  $I_{to}$ . Its reduction when  $I_{to}$  blockade is applied causes a reduction of the outward current and keeps membrane potential higher. Under normal conditions, this “window” current would not be determinant for APD, but in certain pathological conditions or under the effect of drugs that block  $I_{Ks}$ , it may alter the inward/outward current balance of the cell in a way that produces APD prolongation. Thus, the slowdown of  $I_{to}$  inactivation in the modified model produces variations in the membrane potential at the end of phase 1 that indirectly alters the behaviour of  $I_{CaL}$  and  $I_{Kr}$ .

Finally, in the study of Viràg et al. [2], the CL was increased up to 3 s and 0.1  $\mu$ M of dofetilide was used to inhibit  $I_{Kr}$ . These conditions, added to the previous blockades of  $I_{Ks}$  and  $I_{to}$ , resulted in excessive repolarization lengthening and EADs formation. Blockades of 100%, 90% and 55% were applied to  $I_{Ks}$ ,  $I_{to}$  and  $I_{Kr}$ , respectively to reproduce the experiment using the original Decker et al. [4] model. The CL was increased to 3 s and the cells were stimulated until the

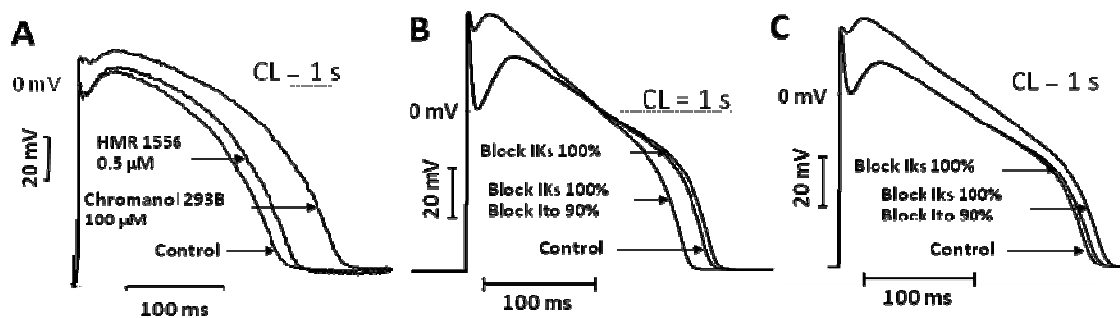
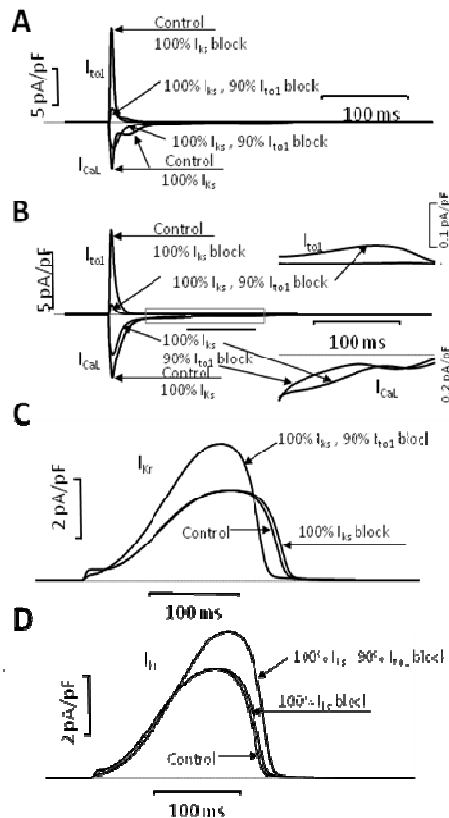


Figure 2. (A) Monitored experimental steady-state APs for a CL of 1 s under control conditions, under the effect of 0.5  $\mu$ M of HMR 1556 and of 100  $\mu$ M of Chromanol 293B added to the previous concentration of HMR 1556. (B y C) Simulated steady-state APs using the original Decker et al. model (B) and the modified model (C) reproducing the effect of MHR 1556 with a blockade of

steady-state. EADs did not appear in the simulations, in contrast to what happened in [2]. When repeating the simulations using the modified  $I_{to}$  model, EADs were found (not shown).



**Figure 3.** Simulated ionic current traces under 90%  $I_{to}$  and  $I_{Ks}$  100% block and in control conditions. (A) Results using the original Decker et al. dog model. Superimposed  $I_{to}$  and  $I_{CaL}$  current traces. (B) Results using the modified Decker et al. dog model. Superimposed  $I_{to}$  and  $I_{CaL}$  current traces. (C) Results using the original Decker et al. dog model.  $I_{Kr}$  current trace. (D) Results using the modified Decker et al. dog model.  $I_{Kr}$  current trace.

The similarities between the ionic currents of dog and human hearts have enabled other studies about the arrhythmogenesis or heart failure using mathematical canine AP models [9, 10]. Despite the Decker et al. [4] model being the most recent model, it failed in reproducing the experimental results found in [2]. Incorporating the new findings of the kinetic of  $I_{to}$  described in this study into the existing dog AP model represents an improvement of the existing knowledge and makes the Decker et al. [4] model more predictive. Furthermore, the current analysis carried out in this work emphasizes the importance of  $I_{to}$  in repolarization and suggests a potential role of  $I_{to}$  blockade in arrhythmogenesis.

## Acknowledgements

This work was partially supported by the European Commission preDiCT grant (DG-INFSo-224381), by the Plan Nacional de Investigación Científica, Desarrollo e Innovación Tecnológica del Ministerio de Ciencia e Innovación of Spain (TEC2008-02090), by the Programa de Apoyo a la Investigación y Desarrollo (PAID-06-09-2843) de la Universidad Politécnica de Valencia, and by the Dirección General de Política Científica de la Generalitat Valenciana (GV/2010/078) and by the Generalitat Valenciana (BEST/2010/102).

## References

- [1] Garfinkel A, Kim YH, Voroshilovsky O, Qu Z, Kil JR, Lee MH et al. Preventing ventricular fibrillation by flattening cardiac restitution. *Proc Natl Acad Sci U S A* 2000; 97(11):6061-6066.
- [2] Varró A, Virág, L. Important role of transient outward current in cardiac repolarization. *Heart Rhythm* 2010, 7(5), Supplement (May 2010), S347, PO5-80.
- [3] Sun X, Wang HS. Role of the transient outward current ( $I_{to}$ ) in shaping canine ventricular action potential—a dynamic clamp study. *J Physiol* 2005; 564(Pt 2):411-419.
- [4] Decker KF, Heijman J, Silva JR, Hund TJ, Rudy Y. Properties and ionic mechanisms of action potential adaptation, restitution, and accommodation in canine epicardium. *Am J Physiol Heart Circ Physiol* 2009; 296(4):H1017-H1026.
- [5] Varro A, Balati B, Iost N, Takacs J, Virag L, Lathrop DA et al. The role of the delayed rectifier component  $I_{Ks}$  in dog ventricular muscle and Purkinje fibre repolarization. *J Physiol* 2000; 523 Pt 1:67-81.
- [6] Hund TJ, Rudy Y. Rate dependence and regulation of action potential and calcium transient in a canine cardiac ventricular cell model. *Circulation* 2004; 110(20):3168-3174.
- [7] Livshitz LM, Rudy Y. Regulation of  $Ca^{2+}$  and electrical alternans in cardiac myocytes: role of CAMKII and repolarizing currents. *Am J Physiol Heart Circ Physiol* 2007; 292(6):H2854-H2866.
- [8] Liu DW, Gintant GA, Antzelevitch C. Ionic bases for electrophysiological distinctions among epicardial, midmyocardial, and endocardial myocytes from the free wall of the canine left ventricle. *Circ Res* 1993; 72(3):671-687.
- [9] Cabo C, Boyden PA. Electrical remodeling of the epicardial border zone in the canine infarcted heart: a computational analysis. *Am J Physiol Heart Circ Physiol* 2003; 284(1):H372-H384.
- [10] Winslow RL, Rice J, Jafri S, Marban E, O'Rourke B. Mechanisms of altered excitation-contraction coupling in canine tachycardia-induced heart failure, II: model studies. *Circ Res* 1999; 84(5):571-586.

Beatriz Carbonell Pascual  
C.P.I. Camino de Vera s/n, 46022  
Valencia (España) Tel: +34 96387751867030  
bcarbonell@gbio.i3bh.es